Effect of Addition of EVA on the Technical Properties of Extruded Foam Profiles of Low-Density Polyethylene/EVA Blends

M. A. RODRÍGUEZ-PÉREZ,[1] A. DUIJSENS,[2] J. A. DE SAJA[1]

[1] Departamento de Física de la Materia Condensada, Cristalografia y Mineralogia, Facultad de Ciencias, Prado de la Magdalena s/n, Universidad de Valladolid, 47011, Valladolid, Spain

[2] Research and Development Department, Sekisui Alveo BV, Postbus 292, 6040 AG Roermond, The Netherlands

ABSTRACT: Some technical properties (static mechanical properties, dynamic mechanical properties, creep-recovery behavior, thermal expansion, and thermal conductivity) of low-density foams (50 kg/m^3) made of blends of low-density polyethylene (LDPE) and the ethylene vinyl acetate copolymer (EVA) were studied as a function of the EVA proportion in the blends. These properties were compared with those of a foam made of a blend of EVA and ethylene propylene rubber (EPR). The knowledge of how the EVA proportion influences the behavior of these blend foam materials is a fundamental factor in order to obtain a wide range of polyolefin foams, with similar density, suitable for different applications. © 1998 John Wiley & Sons, Inc. J Appl Polym Sci 68: 1237–1244, 1998

Key words: polyolefin foams; technical properties of foams; foams with tailored properties; polymer blends

INTRODUCTION

Nowadays, foams are important in the man-made world; the reasons are both technical and commercial. From a technical point of view, a variety of properties, such as light weight, chemical resistance and inertness, buoyancy, good aging, cushioning performance, thermal and acoustic insulation, and recyclability, have ensured that polyolefin foams have penetrated the automotive and transport, building and construction, marine, medical, sports, and leisure markets.

The commercial driving force is cost reduction. Density reduction can be converted directly to cost savings, and it is the reason why commercially produced foams are inexorably being driven toward their lowest possible density for a given application. As densities become lower, the control and optimization of the physical properties becomes more complex. To facilitate the progress in this respect, there is a need for a better understanding of the fundamental relationships between composition, cellular structure, matrix morphology, and physical properties. The published literature contains very few fundamental correlations on these interrelationships for polyolefin foams.

Some comments on the properties of the polymers are necessary to understand the experimental results: Ethylene vinyl acetate (EVA) copolymers with a low VA content, in comparison with LDPE, are more transparent, more flexible, and tougher and have a higher shrinkage at low temperature and a lower thermal conductivity. These materials are used in many flexible items. Blends of polyolefins with ethylene propylene rubbers

Table I Density and Chemical Composition of Materials Used

Materials	Density (kg/m^3)	Chemical Compostion
EVA$_{10}$	49	LDPE 90% EVA 10%
EVA$_{30}$	47	LDPE 70%, EVA 30%
EVA$_{90}$	52	LDPE 10%, EVA 90%
EP$_{25}$	51	EPR 25%, EVA 75%

have been extensively investigated, primarily with the aim of improving tensile and impact properties.

The experimental results show that it is possible to manufacture low-density polyolefin foams with different physical properties, which is an important step for tailoring material properties essential for advanced product design.

EXPERIMENTAL

Materials and Foaming

The densities and chemical compositions (reported by the company) of the industrial materials used in this investigation are summarized in Table I. Three of the foamed industrial samples are made of blends of low-density polyethylene (LDPE) and the EVA copolymer (vinyl acetate content of 12%). Another foam has been made of a blend of EVA and ethylene propylene rubber (EPR with a propylene proportion of 28%). All materials were kindly provided by Alveo (a Sekisui Co., Roermond, The Netherlands).

The materials are physically crosslinked polyolefin foam sheets. In this foaming method, the chains are linked into a network by a high-energy electron beam, which serves to control and stabilize the expansion. After that, the foaming agent in the sheet is activated by heat. Foaming is free, and the foaming process is carried out in a horizontal plane. After the expansion process is completed, the foams are passed through cooling rolls and wound up.

Differential Scanning Calorimetry (DSC)

The thermal properties were studied using a Mettler DSC30 differential scanning calorimeter, calibrated with indium. The weights of the samples were approximately 4 mg, and the experiments were performed in the temperature range from 60 to 200°C with a heating rate of 10°C/min. Each type of sample was scanned three times.

Scanning Electron Microscopy (SEM)

Quantitative image analysis was used to assess the types of cellular structure and apparent mean cell diameter. For this purpose, the cross sections of the extrudate were microtomed at low temperature to provide a smooth surface which, after vacuum coating with gold, was examined by SEM with a JEOL JSM-820 microscope. Each micrograph was analyzed by obtaining data from five reference lines. The apparent mean cell diameter was determined by calculating the number of cells that intersected each reference line and by dividing the appropriate reference line length in the number of cells.[1]

Dynamic Mechanical Analysis (DMA)

Dynamic mechanical testing has long been employed in the study of the viscoelastic response of polymers. In this work, a preliminary study of the influence of the EVA content on the behavior of our samples was performed. The DMA equipment (Perkin–Elmer DMA7) was calibrated according to the recommended procedures using the manufacturer's software. The storage modulus (E'), loss modulus (E''), and loss tangent (tan δ) were obtained in a parallel plate measurement system, a configuration suited for the porous nature of the samples. These properties were measured at the frequency of 1 Hz in the temperature range from −15 to 125°C with a heating rate of 5°C/min. The applied static strain and dynamic strain were chosen in the low strain range (4% static strain and 0.30% dynamic strain), where the mechanism that controls the sample's behavior is the cell wall bending.[2] The plate diameter was 10 mm, and the test specimens were prepared in a cylindrical shape with the same diameter. The thicknesses of the specimens ranged from 8 to 11 mm.

Creep-recovery Measurements

Compressive creep recovery at room temperature (about 24°C) was recorded over a range of applied stresses (σ). The load program applied to the samples is shown in Figure 1(a). All experiments were performed with a plate diameter of 10 mm and samples with a cylindrical shape of the same diameter. The recovery stress (σ_r) was 1.3×10^3 Pa. The creep stresses (σ_c) used were 3.4×10^5, 2.6×10^4, 1.9×10^4, 1.3×10^4, and 7.5×10^3 Pa and the time of the creep and recovery was 20 min.

In Figure 1(b), a typical creep-recovery curve

(a)
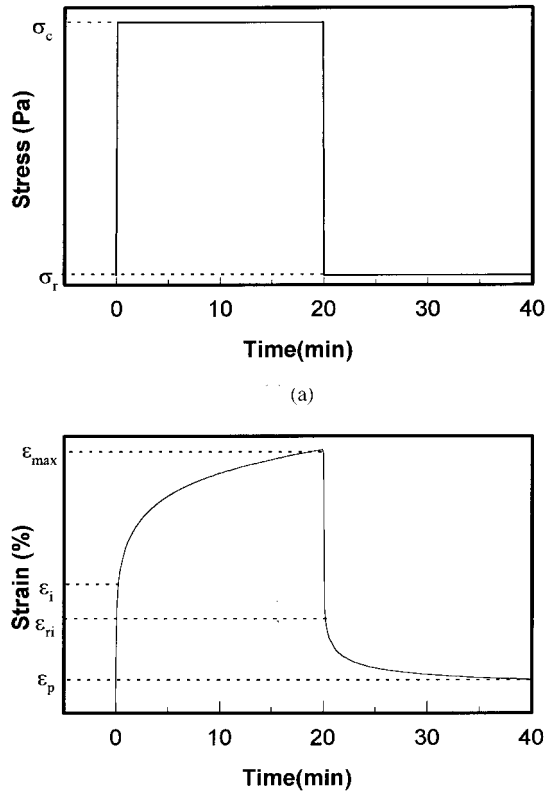
Parameters used to characterize the creep - recovery curve

Strain (%) = ε (t)

ε_i= ε (t=0.1min)

ε_{max}= ε (t=20min)

ε_{ri}= ε (t=20.1min)

ε_p= ε (t=40 min)

(b)

Figure 1 (a) Load program applied to the samples in the creep-recovery experiments. (b) Typical creep-recovery response. The parameters used to described this curve are shown.

of these materials and the parameters used to characterize their behavior are shown. If $\varepsilon(t)$ represents the strain as a function of the time (in minutes), the other parameters were defined as $\varepsilon_i = \varepsilon(t = 0.1 \text{ min})$, $\varepsilon_{max} = \varepsilon(t = 20 \text{ min})$, $\varepsilon_{ri} = \varepsilon(t = 20.1 \text{ min})$, and $\varepsilon_p = \varepsilon(t = 40 \text{ min})$.

The parameters used to compare the response of each sample were defined as

Instantaneous strain:

$$E_i = \frac{\varepsilon_i}{\varepsilon_{max}} 100 \qquad (1)$$

Retarded strain:

$$E_r = \frac{\varepsilon_{max} - \varepsilon_i}{\varepsilon_{max}} 100 \qquad (2)$$

Instantaneous recovery:

$$R_i = \frac{\varepsilon_{max} - \varepsilon_{ri}}{\varepsilon_{max} - \varepsilon_p} 100 \qquad (3)$$

Retarded recovery:

$$R_r = \frac{\varepsilon_{ri} - \varepsilon_p}{\varepsilon_{max} - \varepsilon_p} 100 = 100 - R_i \qquad (4)$$

Plastic strain:

$$E_p = \frac{\varepsilon_p}{\varepsilon_{max}} 100 \qquad (5)$$

Isocronous stress–strain curves were obtained from the experiments to characterize the static mechanical properties of the foams.

Thermal Expansion

The thermal expansion coefficient (α) was measured with a Perkin–Elmer DMA 7 test equipment in the thermomechanical analysis (TMA) mode with an applied stress of 150 Pa, which is sufficient to ensure that the probe remains in contact with the sample, and the compression strain is small enough to be neglected. The tests were performed between −20 and 200°C at the rate of 5°C/min with the same measurement system previously described. The thermal expansion coefficient, between two temperatures T_1 and T_2, was calculated from the usual definition:

$$\alpha = \frac{1}{L_0} \frac{L_1 - L_2}{T_1 - T_2} \qquad (6)$$

where L_0 is the sample height at 24°C, and L_1 and L_2, the sample heights at T_1 and T_2, respectively.

Thermal Conductivity

A Rapid K heat flow meter from Holometrix was used for the thermal measurements. Heat flow through the test sample (q) results from having a temperature gradient (ΔT) across the material. The thermal conductivity λ is defined according to Fourier's equation:
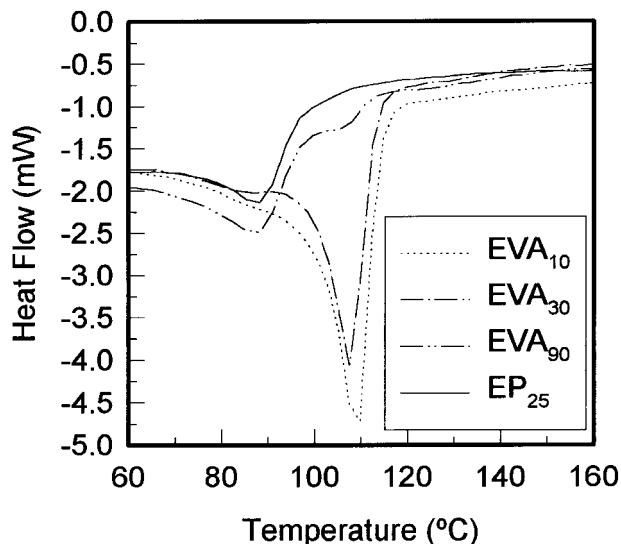
Figure 2 DSC scans of each material.

$$q = \lambda A \frac{\Delta T}{d} \qquad (7)$$

where A is the cross-sectional area of the sample and d is the sample thickness.

The heat flow meter is a thermopile which gives an output of 40 μV for a temperature drop of 1°C. It is a 10-cm-side square which occupies the central portion in the cold face of the equipment. The total face area is a square of 30 cm per side, the remaining portion acting as a shield that keeps the heat flow uniform in the measuring central section. The method is not absolute and therefore needs to be calibrated using a standard sample. Once this has been done, the heat flow per unit area can be found from the reading of the heat flow transducer, and the thermal conductivity of the sample can thus be calculated using eq. (7).

The measurements were made under steady heat flow conditions through the test sample. These were done in accordance with ASTM C518 and ISO DIS 8301 methods. Square samples of 30 cm per side and 8-mm thickness were used for all experiments. A dispersion of less than 1% in two consecutive readings was taken as a criterion to ensure that the measurements were done under steady-state conditions. The time step between readings was 10 min. The measurements were performed at 24°C, and each experiment was repeated five times in order to obtain an average value. The precision of the apparatus was approximately 5%.

Density

Foam samples were conditioned at 24°C and 50% relative humidity for 24 h and subjected to density measurements in accordance with ASTM D1622.

RESULTS

DSC and SEM

The morphology of the samples was determined using these techniques, focusing the study on some of the characteristics that play a fundamental role in the physical behavior of the foams. The DSC scans of the EVA/LDPE blend foams are summarized in Figure 2. Figure 2 shows that the blend foams have the typical behavior of continuous polymer blends (where intermixing at the molecular level rarely occurs[3]) with one endothermic peak for each polymer in the blend. The first peak (85°C) is associated with the EVA content, and the second one (107°C), with the LDPE content. From that figure, it is clear that foams with a low EVA percentage have a higher thermal stability.

The mean estimated values for the basic parameter that characterizes the cellular structure, the cell diameter, are given in Table II. All foams present a closed-cell structure with cells almost spherical (some micrographs of these materials can be seen in Fig. 3). The cell size is similar for all the foams, except for the EVA$_{90}$ material which presents larger cells.

Technical Properties

Isocronous stress–strain curves (time of creep 20 min) are plotted in Figure 4. From Figure 4, the static modulus (E), defined as the slope of the stress/strain curve within the linear region, was calculated, and the results are given in Fig. 5(a). Figure 5(a) shows that the static modulus decreases linearly with the EVA content. On the other hand, the EP$_{25}$ material has a lower static

Table II Mean Cell Diameters of Materials Used

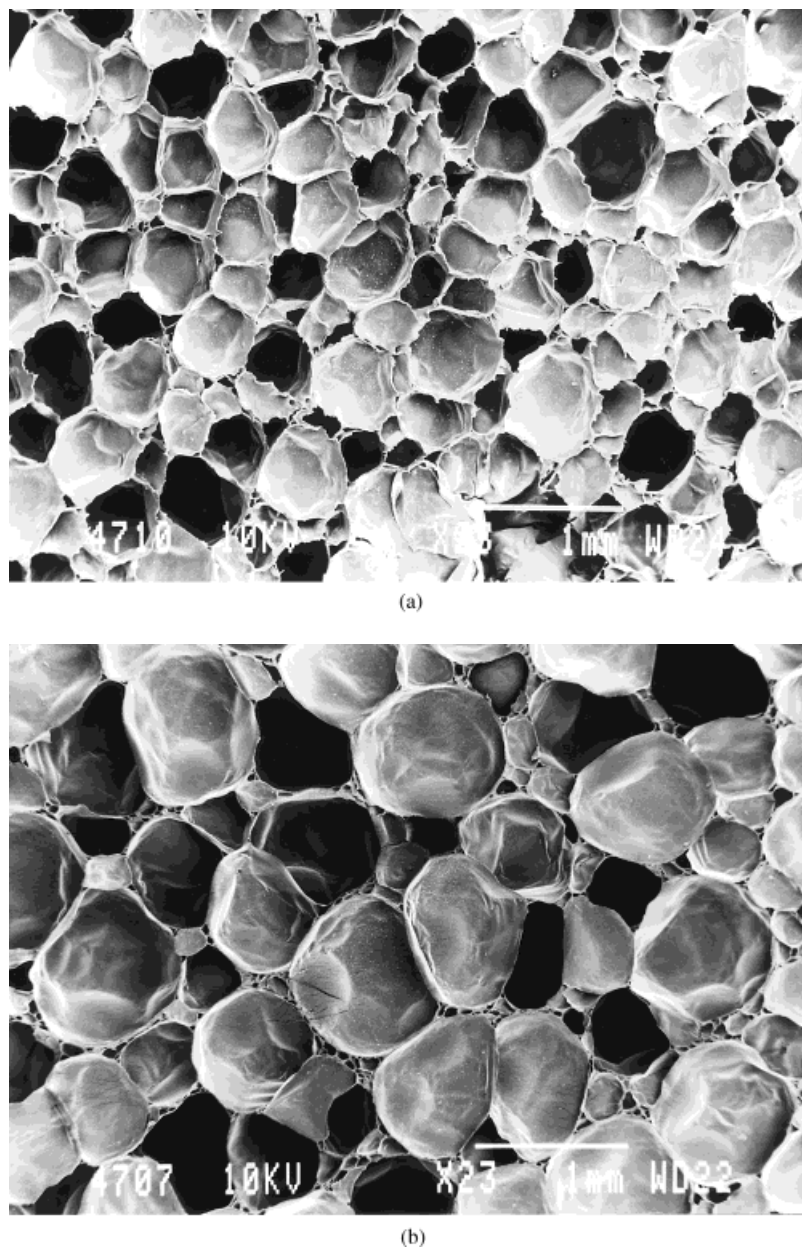| Materials	Mean Cell Diameter (μm)
EVA$_{10}$	340
EVA$_{30}$	320
EVA$_{90}$	540
EP$_{25}$	330

Figure 3   SEM micrographs of two foams: (a) EVA_{10}; (b) EVA_{90}.

modulus than that of a blend of LDPE/EVA with the same EVA content (75%).

The parameters that characterize the deformation and recovery behavior are shown in Figure 5(b) for experiments with $\varepsilon_{max} = 10\%$. Figure 5(b) shows that while the instantaneous recovery increases linearly with the EVA content the retarded recovery and the plastic strain decreases with it. The instantaneous deformation also increases with the EVA content.

The EP_{25} foam has the best instantaneous recovery, and its plastic strain has the same order

as that of the other materials. Furthermore, its instantaneous deformation is the highest.

In the range of the deformation studied (low strains), it is well known[4,5] that the absorption capabilities of the foam materials are controlled mainly by the viscoelasticity of the material in the cell walls. Figure 6(a,b) represents the viscoelastic response of the samples.

These materials are blends of EVA and LDPE, and due to this reason, the tan δ curve presents the typical behavior of an LDPE sample[6] (for the materials with a high LDPE content) and the typ-
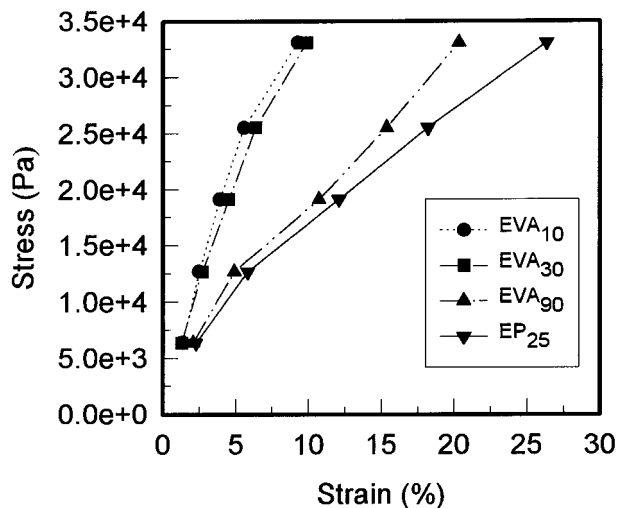
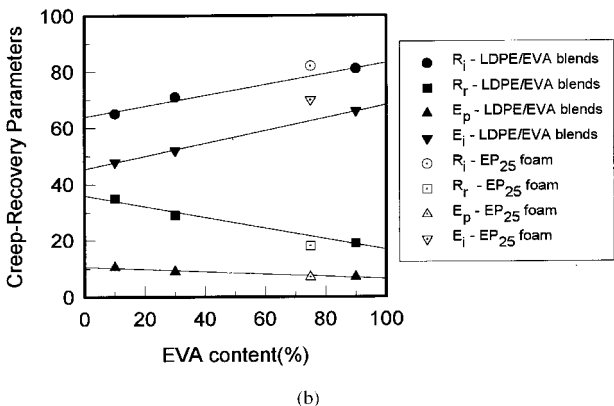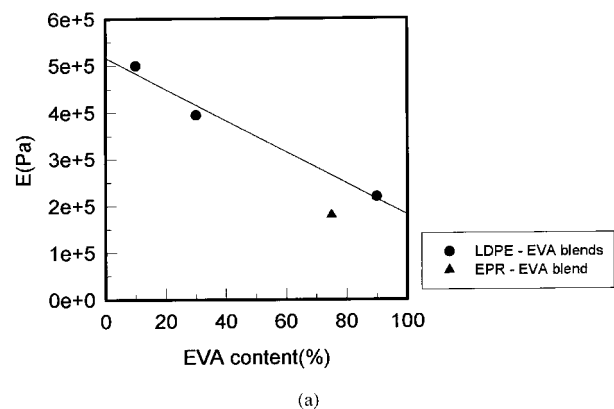**Figure 4** Isocronous stress–strain curves for a time of creep of 20 min.

(a)

(b)

Figure 5 (a) Static modulus as a function of the EVA proportion in the blends. The static modulus of the EP_{25} material is also shown. (b) Instantaneous strain, instantaneous recovery, retarded recovery, and plastic strain as a function of the EVA content for the LDPE/EVA blends and for the EP_{25} material.
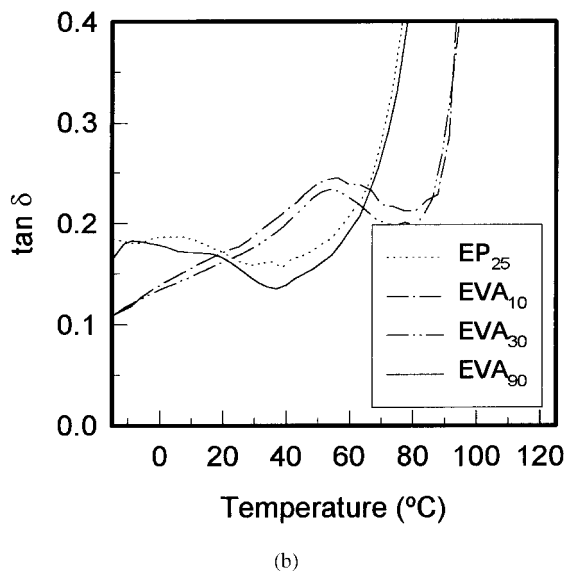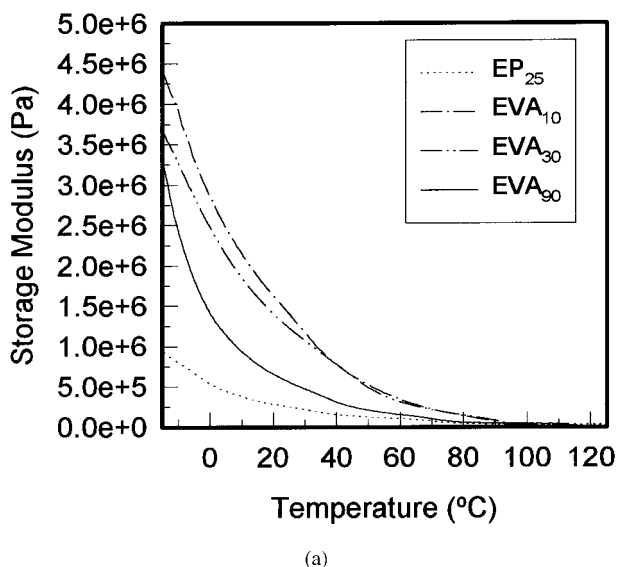

(a)

(b)

Figure 6 (a) Storage modulus (E') as a function of the temperature. (b) Loss factor $(\tan \delta)$ as a function of the temperature.

ical behavior of an EVA sample[7] (for the materials with a high EVA content). For a material with an intermediate proportion, the viscoelastic response would be intermediate between the behaviors of the two polymers. On the other hand, the storage modulus, loss modulus, and loss tangent, at room temperature, decrease linearly with the EVA content and have the same behavior as that of the static modulus. The loss factor at 25°C as a function of the EVA content is plotted in Figure 7(a).

From an applied point of view, with these blends, it is possible to obtain materials with a higher damping factor at low temperatures (high

EVA content) and with a higher damping factor at high temperatures (low EVA content). If the time–temperature superposition principle is applied, the previous results indicate that it is possible to have materials with a good response in a broad range of frequencies for applications at room temperature.

The EP_{25} foam has a lower storage modulus than that of the LDPE/EVA blend foams with a higher EVA content. The tan δ value at room temperature is higher than that of an LDPE/EVA blend foam with the same EVA content.

The thermal expansion calculated between 25 and 30°C is plotted in Figure 7(b). Figure 7(b) shows that the thermal expansion also follows a linear relationship with the EVA content and increases as the EVA content increases. The EP_{25} foam material has a higher thermal expansion than that of the LDPE/EVA blend foam with the same EVA content.

On the other hand, a different result can be obtained when the thermal conductivity is studied. There is no clear behavior of the thermal conductivity as a function of EVA content [Fig. 7(c)]. This could be due to the strong influence of cell size on the thermal conductivity[8,9] and to the different cell sizes of the samples. The materials have different cell sizes, and the effect of this parameter on the thermal conductivity can be bigger than the effect of the polymer blend on the cell walls.

In short, all properties described above (except thermal conductivity) follow a linear relationship with the EVA content in the blends (the linear fits are given in Table III). Foams with similar density have different properties if the cell faces are made of different polymers. In the LDPE/EVA blend foams, the final properties are controlled by the EVA content in the cell faces. The trends of the properties are similar to those of continuous (noncellular) LDPE/EVA blends.

This happens in all properties that are almost independent of cell size,[2] but for the thermal conductivity (which is strongly dependent of cell size), the previous trends do not come true due to the different cell diameters of the samples.

Figure 7 (a) Loss factor at 25°C as a function of the EVA content in the blends. The tan δ value for the EP_{25} material is also shown. (b) Thermal expansion, between 25 and 30°C, as a function of the EVA proportion in the blends. The behavior of the EP_{25} material is also plotted. (c) Thermal conductivity as a function of the EVA content for the LDPE/EVA blends and for the EP_{25} material.
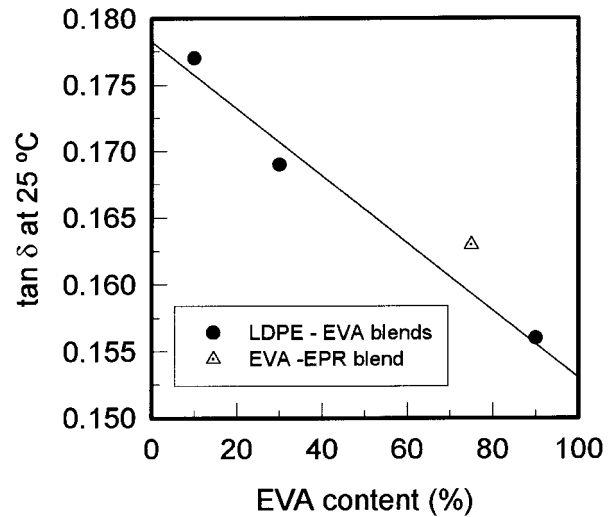
(a)
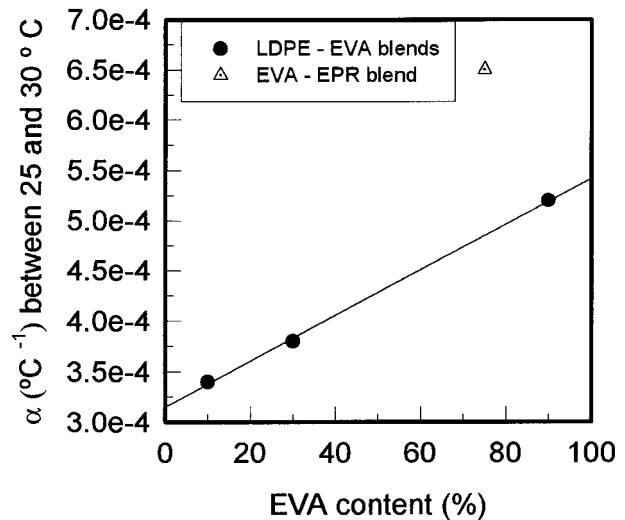
(b)
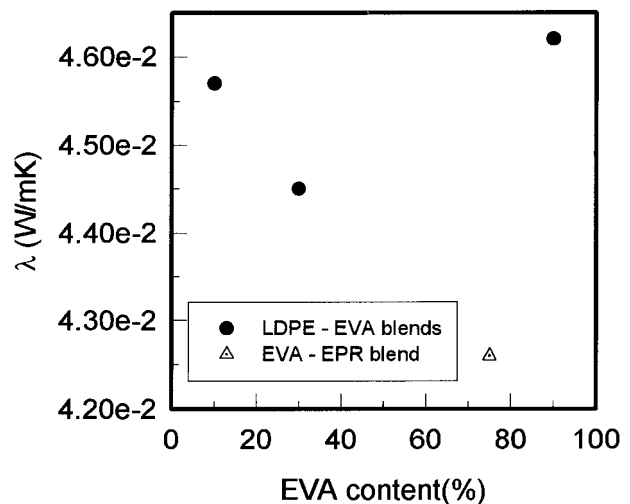
(c)

Table III   Linear Fits with EVA Content

Property = $a + b$ [EVA Content (%)]	a	b	r^2
Static modulus (Pa)	5.4×10^5 (Pa)	4446 (Pa/%)	0.996
R_i (%)	64 (%)	0.192 (%/%)	0.981
R_r (%)	36 (%)	-0.192 (%/%)	0.981
E_p (%)	10.6 (%)	-0.041 (%/%)	0.983
E_i (%)	45.5 (%)	0.227 (%/%)	0.999
E' at 25°C (Pa)	1.53×10^6 (Pa)	-1.08×10^4 (Pa/%)	0.998
E'' at 25°C (Pa)	2.7×10^5 (Pa)	-2012 (Pa/%)	0.999
Tan δ at 25°C	0.178	-2.52×10^{-4}	0.979
α (°C^{-1})	3.15×10^{-4} (°C^{-1})	2.27×10^{-7} (°C^{-1}/%)	0.999

On the other hand, the EP_{25} material presents different properties compared with that of a blend of EVA/LDPE with the same EVA content. From an applied point of view, it would be possible to make another group of foams with different properties with the change of the EVA content in the blends.

CONCLUSIONS

Several technical properties of crosslinked closed-cell polyolefin foams made of blends of LDPE and EVA were studied in terms of the EVA proportion in the blends. The properties of these blends were also compared with those of a blend of EVA and EPR with similar density.

The results have shown that it is possible to extend the range of properties of LDPE foams by blending them with EVA, which is an important step in obtaining materials with tailored properties, essential for advanced product design.

It was also shown that the static and dynamic modulus and the thermal stability decreases when the EVA content increases, while instantaneous recovery, thermal expansion, and the loss factor at low temperatures increases as the EVA content increases.

Other observations have shown that all properties change linearly (except thermal conductivity) with the EVA proportion. Foams with similar density have different properties if the cell faces are made of different polymers. In the blend foams, the final properties are controlled by the EVA proportion in the cell faces. This happens in all the properties that are almost independent of the cell size, but for the thermal conductivity (which is well known to be strongly dependent on the cell size), the previous trends do not come true due to the different cell diameters of the samples. For the thermal conductivity, the control of the cell size is of the same importance as the chemical composition in the cell walls.

The EP_{25} foam has different properties due mainly to the effect of the EPR on the properties of the cell walls. This foam is more flexible and has a lower thermal conductivity, a lower static and storage modulus, and a higher loss factor.

REFERENCES

1. G. L. A. Sims and C. Khunniteekoll, *Cell. Polym.,* **13,** 137 (1994).
2. L. J. Gibson and M. F. Ashby, *Cellular Solids: Structure and Properties,* Pergamon Press, Oxford, 1988.
3. D. Campbell and J. R. White, *Polymer Characterisation, Physical Techniques,* Chapman and Hall, London, 1989.
4. N. C. Hylard and A. Cunningham, *Low Density Cellular Plastics. Physical Basis of Behaviour,* Chapman and Hall, London, 1994.
5. M. A. Rodríguez-Pérez, S. Rodríguez-Llorente, and J. A. de Saja, *Polym. Eng. Sci.,* **37,** 959 (1997).
6. N. Alberola, J. Y. Cavaille, and J. Pérez, *J. Polym. Sci. Polym. Phys. Ed.,* **28,** 569 (1990).
7. R. Popli, M. Glotin, L. Mandelkern, and R. S. Berson, *J. Polym. Sci. Polym. Phys. Ed.,* **22,** 407 (1984).
8. A. G. Leach, *J. Phys. D Appl. Phys.,* **26,** 733 (1993).
9. M. A. Rodríguez-Pérez, O. Alonso, J. Souto, and J. A. de Saja, *Polym. Test.,* **16,** 287 (1997).